Solid Acid Catalyst WO_3-ZrO_2 for the Catalytic Deoxygenation of Jatropha Oil for the Preparation of Aviation Paraffin

Jiayu Lin,[a] Jin Li,[a,*] Shiyun Zhou,[a] Yang Cao,[b] Shurong Wang,[a] and Jiao Jiang [a]

WO_3-ZrO_2 solid acid catalysts were prepared by the impregnation method and characterized by X-ray diffraction (XRD), transmission electron microscope (TEM), Brunauer-Emmett-Teller (BET), and pyridine adsorbed IR spectroscopy (Py-IR). The catalysts were used for catalytic deoxygenation of *Jatropha curcas* oil. The optimal conditions for the deoxygenation of the generated oil were obtained by response surface methodology based on Box-Behnken four-factor experiments. Response surface methodology (RSM) was applied while determining the optimal conditions for the Jatropha oil deoxygenation percentage. The rate was calculated based on Box-Behnken four-factor experiments, with reaction temperature, catalyst amount, reaction time, and reaction pressure as independent variables and the deoxygenation of Jatropha curcas oil as response values. The optimal reaction conditions obtained were a temperature of 370 °C, pressure of 2 MPa, time of 7 h, and catalyst amount of 0.22 g. The deoxygenation percentage of the generated oil under the optimal conditions was 95.1%, which was close to the theoretical value, indicating that the model was reliable. The generated oil contained more jet fuel components, with 68.1% C8-C16, 12.0% isoalkanes, 14.2% cycloalkanes, and 8.9% aromatic compounds under the optimum conditions. This study provides an effective and simple method for preparation of bio-aviation fuel.

DOI: 10.15376/biores.17.4.5679-5694

Keywords: WO_3-ZrO_2; Jatropha oil; Catalytic deoxygenation; Response surface methodology

Contact information: a: College of Chemical Engineering and Technology, Hainan University, Haikou 570228, Hainan, China; b: Qiongtai Normal University, Haikou 571127, China;
** Corresponding author: 316800681@qq.com*

INTRODUCTION

Global energy consumption is projected to rise to 50% by 2050 (Kim *et al.* 2021). The increasing use of fossil energy sources leads to gigantic amounts of greenhouse gas emissions and a series of environmental problems (Xu *et al.* 2018; Wang 2019). Research in exploring the application of biomass energy has continuously gained importance due to the shortage of fossil energy and the rise of crude oil prices (Yang and Dian 2022). Meanwhile, as one of the major fossil energy source consumers, the air transport industry urgently requires a more efficient and economical alternative source of energy to achieve a sustained and rapid development, which creates a promising prospect for biofuels usage (Nygren *et al.* 2009). Non-edible fats and oils for bio-airline kerosene development can reduce the dependence on petrochemical energy, and they have significance for improving the environment and increasing farmers' income (Islam *et al.* 2018; Doliente *et al.* 2020). Jatropha oil is widely distributed in most parts of the world, such as Africa, Australia, the

United States, China, India, and so on (Kumar *et al.* 2010; Verma *et al.* 2015). To partially replace the traditional fuel consumption and reduce the pressure of fossil energy, biofuels development is in urgent demand. Jatropha oil is considered as a promising alternative for sustainable energy. For meeting the requirements of aviation fuel, our team converted Jatropha oil into hydrocarbons through catalytic deoxygenation.

The deoxygenation pathways of biomass oil are mainly decarbonylation (DCO), decarboxylation (DCO_2), and hydrodeoxygenation (HDO) (Gosselink *et al.* 2013; Stepacheva *et al.* 2021). These HDO reactions of bio-oil are enhanced by noble metals such as Pd, Pt, Rh, and Ru, which are mainly supported on carbon, in addition to ZrO_2, CeO_2 and TiO_2, which also show high HDO activity (Mortensen *et al.* 2011; Wang *et al.* 2013; Zacher *et al.* 2014; Patel and Kumar 2016), but its high cost limits its industrial application. Researchers have focused their efforts on transition metal catalysts in order to find catalysts that can replace sulfide catalysts and reduce the use of precious metal catalysts. Zhu *et al.* (2021) prepared CNi/bentonite catalysts and used them for partial hydrogenation of jatropha oil, which significantly improved the oxidative stability of biodiesel with a mass conversion ratio of C18:2 up to 75%. Yang *et al.* (2021) synthesized a series of Pt/SAPO-11-γ-Al_2O_3 catalysts with excellent coke resistance for the deoxygenation reaction of jatropha oil. These approaches provided an effective strategy for refining bio-airline fuel. Tang *et al.* (2022) prepared a series of NiMoP catalysts with different carriers to investigate the hydrodeoxygenation (HDO) reaction of jatropha oil reaction pathway and catalytic mechanism. WO_3-ZrO_2 is an emerging solid acid catalyst that does not lose acidic components during use because it does not contain elements such as chlorine (Cl) and sulfur (S). It has good thermal stability. Wang *et al.* (2020b) prepared a series of Ni-Cu catalysts loaded on WO_3-ZrO_2 for the hydroisomerization of isobutane to n-butane. The loading of Ni-Cu alloy increased the number of acidic sites and improved the stability and selectivity of the catalyst for n-butane. Zerva *et al.* (2021) investigated the use of 10% Ni/ZrO_2 for HDO experiments of phenol, while adding WO_3 to ZrO_2 to enhance the acidity and successfully achieved complete hydrodeoxygenation of phenol and was able to generate cyclohexane at low temperature (150 °C). Most of the current research on solid acid catalysts has been mainly applied to reactions such as esterification reactions, isomerization of alkanes, and photocatalytic reactions (Lee *et al.* 2017; Samy *et al.* 2020; Shkurenok *et al.* 2021), with less application in actual bio-oils.

In this paper, WO_3-ZrO_2 solid acid catalysts were prepared by the impregnation method. The prepared catalyst was thereafter characterized by X-ray diffraction (XRD), transmission electron microscope (TEM), Brunauer-Emmett-Teller (BET), and pyridine adsorbed IR spectroscopy (Py-IR) and used for the catalytic deoxygenation of *Jatropha curcas* oil. By response surface methodology, four conditions of reaction temperature, reaction pressure, reaction time, and catalyst amount were optimized, and the possible causes of component content and formation in the resulting oil were evaluated.

EXPERIMENTAL

Reagents and Instruments

Jatropha curcas oil was provided by the Hainan Danzhou Jatropha Oil Processing Plant. Ammonium metatungstate hydrate and zirconium hydroxide (IV) were purchased from Shanghai Maclean Biochemical Technology Co., Ltd. (Shanghai, China). Nitrogen (N_2, 99.999% v/v) and hydrogen (H_2, 99.999% v/v) were supplied by Haikou Jiateng

Chemical Gas Co. (Haikou, China). The YZMR-2-100-D(M) Parallel Autoclave was supplied by Shanghai Yanzheng Instruments Co., Ltd. (Shanghai, China).

Catalyst Preparation

First, 0.43 g of ammonium metatungstate hydrate was added to 10.00 g of ultrapure water and stirred to dissolve. Next, 3.00 g of zirconium hydroxide (IV) was added to the aqueous ammonium metatungstate solution, macerated, stirred at room temperature for 12 h. Finally, the material was dried in an oven at 110 ℃ for 12 h, ground, and calcined in a muffle furnace at 800 ℃ for 3 h to obtain the catalyst WO_3-ZrO_2.

Catalytic Deoxygenation Reaction Experiment

All experiments were carried out in a stainless steel high-pressure parallel reactor equipped with a mechanical stirrer and an automatic temperature control system. The jatropha oil and the catalyst were mixed evenly in the autoclave at a ratio of 50:1, and the air in the reactor was replaced by nitrogen. This was repeated three times, and the nitrogen in the reactor was replaced by hydrogen, which also was repeated three times. After the replacement gas was exhausted, the air-tightness of the autoclave was checked by feeding H_2 again for 20 min. Finally, the pressure required for the reaction was fed, and the reaction temperature and time required for the experiment were set, and the rotation speed was set at 500 rpm. After the reaction was completed, the autoclave was rapidly cooled to room temperature, and the resulting oil was centrifuged. The resulting oil was filtered through a 0.45 μm filter membrane and analyzed by GC-MS.

Characterization Methods

XRD was performed for the physical phase identification of the catalyst, operating at 40 kV, 100 mA, and a large angle test rate of 10°/min (D8 Advance x-ray diffractometer, Bruker, Karlsruhe, Germany). TEM was used to characterize the morphology of the catalyst, operating at 200 kV (FEI Tecnai G2 F20 S-Twin 200kV transmission electron microscope, Hillsboro, OR, USA). The surface area and pore size distribution of the catalyst were determined by Brunauer-Emmett-Teller method (Li *et al*. 2020). Py-IR test conditions were vacuum treatment at 350 ℃ for 2 h, adsorption of pyridine saturated vapor at room temperature for 30 min, then programmed to 200 ℃ to desorb pyridine, followed by programmed heating to 350 ℃ to desorb pyridine (PE FT-IR frontier pyridine infrared absorption test, PerkinElmer, Waltham, USA). GC-MS analysis of the resulting oil was performed using an HP-5MS column with test conditions of holding at 50 ℃ for 5 min, a splitting ratio of 20:1 and a carrier gas flow rate of 1 mL/ min, ramped up to 300 ℃ at 60 ℃/min and held for 5 min (7890A-7000B gas chromatograph mass spectrometer, Agilent Technologies, Santa Clara, USA).

The selectivity of deoxygenation products (S_o) and C_{x1}-C_{xn} in *Jatropha curcas* oil was determined by using Eqs. (1) and (2).

$$S_o\ (\%) = (W_2/W_1) \times 100\ \% \quad (1)$$

$$S_{Cx1\text{-}Cxn}\ (\%) = (W_{Cx1\text{-}Cxn}/W_1) \times 100\ \% \quad (2)$$

where W_1 is the total peak area of all compounds in the generated oil, W_2 is the sum of peak areas of the non-oxygenated compounds in the generated oil, and $W_{Cx1\text{-}Cxn}$ is the sum of peak areas of compounds with carbon chain lengths x_1 though x_n.

RESULTS AND DISCUSSION

Catalyst Characterization

XRD analysis

Figure 1 shows the XRD pattern of the prepared WO_3-ZrO_2 catalyst. The WO_3-ZrO_2 catalyst was synthesized after calcination at 800 ℃. Comparison of the sample spectra with PDF standard cards (80-0784 and 72-1465) showed characteristic diffraction peaks for the tetragonal phase ZrO_2 at 2θ=30.24°, 35.27°, 50.26°, and 60.20°. The characteristic diffraction peaks for the WO_3 crystals were 2θ=23.15°, 23.61°, and 24.37°. When the WO_3 loading was 15%, the ZrO_2 crystals were in tetragonal crystalline phase, and the presence of WO_3 inhibited the transformation of $Zr(OH)_4$ to monoclinic crystalline phase ZrO_2 due to water loss during calcination. Thus, the formed ZrO_2 was all in tetragonal crystalline phase (Tong *et al.* 2016).

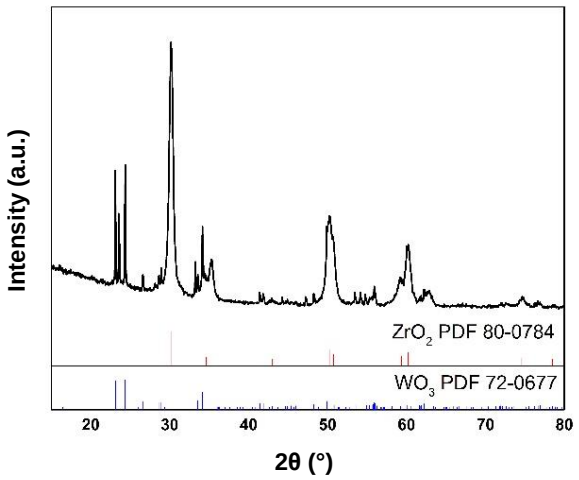

Fig. 1. XRD pattern of WO_3-ZrO_2 catalyst

TEM analysis

Figure 2 shows the TEM image of 15% WO_3-ZrO_2 obtained by roasting at 800 ℃. $Zr(OH)_4$ was in a granular crystalline state after roasting at 800 ℃.

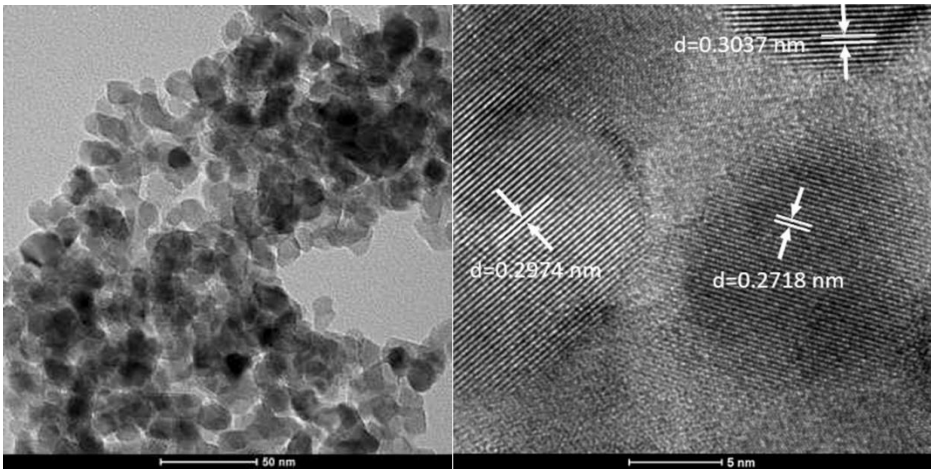

Fig. 2. TEM and HRTEM image of WO_3-ZrO_2

The prepared tungsten-zirconium oxides were all nanoscale, with less agglomeration of particles and more sparsely dispersed. Clearly ordered lattice intervals were observed under the high-resolution images, with a uniformly ordered surface topology and lattice gap widths of 0.2718 to 0.3037 nm.

BET analysis

Figure 3 shows the N_2 isothermal adsorption-desorption curve of 15% WO_3-ZrO_2. The results showed a type IV adsorption isotherm with an H3 hysteresis loop, which was classified as a mesoporous material according to IUPAC. No adsorption saturation was observed at higher pressures (Jing *et al.* 2009), which was probably due to the buildup of nanomaterials, corresponding to Fig. 3. The specific surface area, pore capacity and pore size of the samples were calculated from the BET and BJH equations to obtain Table 1. The 15% WO_3-ZrO_2 prepared in this paper had a better specific surface area, larger pore capacity, and moderate pore size compared to WO_3-ZrO_2 prepared in other literature.

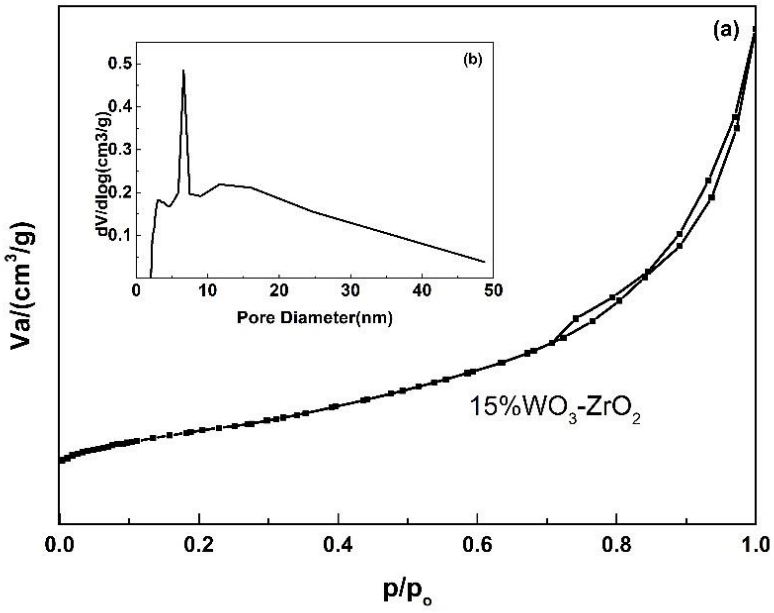

Fig. 3. (a) N_2 isotherm adsorption-desorption curve and (b) pore size distribution of WO_3-ZrO_2

Table 1. N_2 Adsorption and Desorption Data of 15% WO_3-ZrO_2

Samples	S_{BET} (m_2/g)	V_{BJH} (cm_3/g)	D_{BJH} (nm)
ZrO_2 (Pattnaik *et al.* 2021)	93.50	-	6.50
WO_3-ZrO_2 (Pattnaik *et al.* 2021)	56.60	-	11.60
m-ZrO_2 (Salgado *et al.* 2021)	56.00	0.28	19.00
10% WO_3-ZrO_2 (Salgado *et al.* 2021)	82.00	0.21	9.90
WO_3-ZrO_2 (Wang *et al.* 2020a)	67.69	0.12	7.60
WO_3-ZrO_2 (Dedsuksophon *et al.* 2011)	92.00	0.19	3.40
15 % WO_3-ZrO_2 (Present study)	84.42	0.35	10.60

Py-IR analysis

Figure 4 shows the pyridine-adsorbed region of the infrared spectrum of WO_3-ZrO_2. The IR peaks were assigned to pyridine molecules containing Brönsted and Lewis acid sites: 1541 cm^{-1} (BAS), 1488 cm^{-1} (BAS or LES), and 1446 cm^{-1} (LES) (Lercher *et al.* 1996; Halim *et al.* 2009). Similar to what was reported in literature (Jing *et al.* 2009), the pyridine infrared adsorption of ZrO_2 was only composed of the band at about 1450 cm^{-1}, indicating that the introduction of WO_3 introduced the Brönsted acid sites to ZrO_2. The number of Brönsted acid sites depends directly on the WO_3 content (Piva *et al.* 2020).

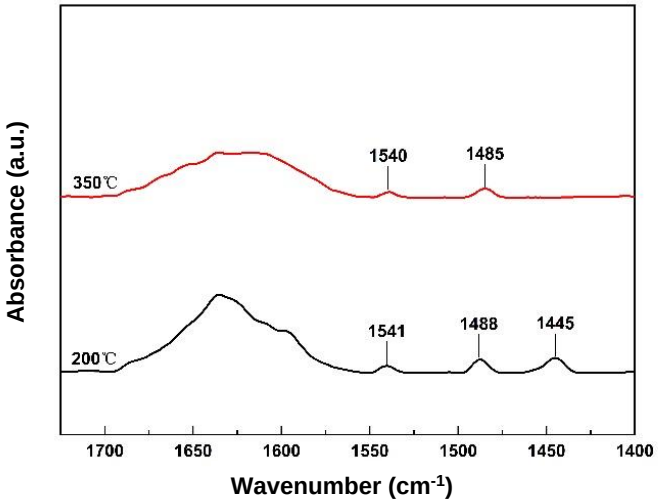

Fig. 4. WO_3-ZrO_2 weight normalized IR spectrum (pyridine IR region)

Table 2 shows the detailed characterization data for the quantification. Brönsted and Lewis acids were present simultaneously at 200 ℃, and the peak intensity showed more Lewis acid sites than Brönsted sites. At 350 ℃ the Lewis acid peak decreased sharply to none, while the Brönsted acid peak decreased slightly. The results indicate a moderate acid intensity at the Lewis site on WO_3-ZrO_2 and a strong acid intensity at the Brönsted site, which suggests a synergistic effect between the Brönsted and Lewis acid sites in WO_3-ZrO_2. The intensity of each peak is proportional to the concentration of the particular type of surface acid site.

Table 2. Acidity Properties of WO_3-ZrO_2

200 °C/(mmol/g)		350 °C/(mmol/g)	
Brönsted	Lewis	Brönsted	Lewis
0.0078	0.0173	0.0056	0.0000

Experimental Analysis of the Box-Behnken Design

Experimental design and results

According to the Box-Behnken design principle, the four factors of reaction temperature (A), reaction pressure (B), reaction time (C), and catalyst amount (D) were selected as independent variables to design response surface orthogonal experiments with the deoxygenation percentage of *Jatropha curcas* oil as the test index. The experimental

components were 24 factor analysis test groups and 5 error estimation test groups. The experimental factors and levels were designed as shown in Table 3, and the experimental sequence was randomized to reduce the influence of uncontrollable factors (Abdulgader *et al.* 2019). The experimental design and results are shown in Table 4.

Table 3. Coding Levels of the Factors in the Experimental Design

Factors	Variables		Level	
		-1	0	1
Reaction temperature (°C)	A	350	360	370
Reaction pressure (MPa)	B	2	3	4
Reaction time (h)	C	4	6	8
Amount of catalyst (g)	D	0.1	0.2	0.3

Table 4. Response Surface Experimental Design and Results

Serial Number	Level				Deoxygenation (%)
	Reaction Temperature (°C)	Reaction Pressure (MPa)	Reaction Time (h)	Catalyst Amount (g)	
1	350	2	6	0.2	84.68
2	370	2	6	0.2	94.97
3	350	3	6	0.3	85.73
4	360	3	6	0.2	92.28
5	360	2	6	0.3	92.28
6	350	4	6	0.2	86.67
7	360	3	6	0.2	92.33
8	360	4	4	0.2	92.15
9	360	2	4	0.2	91.55
10	370	3	6	0.1	93.76
11	360	3	4	0.1	91.02
12	360	4	8	0.2	92.57
13	360	4	6	0.1	92.14
14	370	3	4	0.2	93.87
15	360	4	6	0.3	93.35
16	350	3	4	0.2	85.25
17	370	3	6	0.3	94.72
18	360	3	8	0.1	91.97
19	350	3	8	0.2	86.48
20	360	3	8	0.3	92.53
21	360	2	8	0.2	92.91
22	360	3	6	0.2	92.85
23	370	3	8	0.2	94.17
24	370	4	6	0.2	93.85
25	360	2	6	0.1	92.13
26	360	3	6	0.2	93.60
27	360	3	6	0.2	92.99
28	360	3	4	0.3	92.21
29	350	3	6	0.1	85.06

Regression equation and parameter analysis

Based on the Box-Behnken design principle, the deoxygenation percentage of the resulting generated oil was made to fit the generated oil deoxygenation percentage (Y) and the variables to each other through multiple regressions by Design-Expert 8.0.6.1 software (Xiao *et al.* 2021). Design-Expert 8.0.6.1 software determined and evaluated the coefficients and statistical significance of the complete regression model equation to establish the effect of Y on quadratic mathematical models for reaction temperature (A), reaction pressure (B), reaction time (C), and catalyst amount (D), with positive signs before each coefficient indicating synergistic effects and negative signs indicating antagonistic effects. The quadratic mathematical regression equation is as follows.

$$Y=92.81+4.29\ A+0.18\ B+0.38\ C+0.39\ D-0.78\ AB-0.23\ AC+0.072\ AD-0.24\ BC+0.26\ BD-0.16\ CD-2.59\ A^2-0.083\ B^2-0.40\ C^2-0.38\ D^2$$

As shown in Table 5, the reliability of the model can be obtained from the coefficient of variation, which is negatively correlated with the reliability, with an upper limit of 10%.

Table 5. Mathematical Model R^2 Regression Analysis

Coefficient of Variation (%)	R^2	R^2 Calibration Values	R^2 Predicted Values	Signal to Noise Ratio
0.39	0.9935	0.9869	0.9803	39.376

Table 6. Mathematical Model Analysis of Variance

Source of Variance	Sum of squares	Freedom	Mean Square	F-value	P-value	Significance
Model	272.62	14	19.47	152.08	< 0.0001	Significant
A	220.76	1	220.76	1724.13	< 0.0001	
B	0.41	1	0.41	3.18	0.0963	
C	1.75	1	1.75	13.65	0.0024	
D	1.87	1	1.87	14.62	0.0019	
AB	2.42	1	2.42	18.88	0.0007	
AC	0.22	1	0.22	1.69	0.2148	
AD	0.02	1	0.02	0.16	0.6914	
BC	0.22	1	0.22	1.73	0.2101	
BD	0.28	1	0.28	2.19	0.1607	
CD	0.10	1	0.10	0.77	0.3936	
A^2	43.44	1	43.44	339.28	< 0.0001	
B^2	0.04	1	0.04	0.35	0.5645	
C^2	1.06	1	1.06	8.28	0.0122	
D^2	0.92	1	0.92	7.19	0.0179	
Residuals	1.79	14	0.13			
Loss of proposed items	0.62	10	0.06	0.21	0.9784	Not significant
Error term	1.17	4	0.29			
Total error	274.41	28				

The coefficient of variation of the generated oil deoxygenation percentage in this experiment was 0.39%, which indicates a high reliability. R^2 is the fit of the quadratic mathematical model of the reaction, and the closer the R^2 value is to 1, the better the fit is. The average prediction error of the model can be seen from the signal-to-noise ratio data, and the lower limit is 4. The signal-to-noise ratio of this experiment was 39.376, and the model fits well within the designed range.

The variance data for the response surface quadratic mathematical model are shown in Table 6, and the significance of the model and factors were examined using P values, with $P<0.05$ being a significant effect and $P<0.01$ being very high significance (Qian *et al.* 2014). The model p-value < 0.0001, the model regression term was significant, and the out-of-fit to $P=0.9784>0.05$ was not significant, indicating that the experimental results fit well with the mathematical model.

The F-value indicates that the response surface data can be illustrated by the data of the regression equation. The larger the F-value indicates more significant results, and when the F-value increases to a certain value ($P<0.0001$), the stronger the linear correlation is demonstrated. By analysis, the order of influence of the four factors on the deoxygenation percentage of the generated oil was reaction temperature > catalyst amount > reaction time > reaction pressure.

Response surface analysis

The three-dimensional response surface diagram can visually display the trend of the influence of the interaction of different influencing factors on the response value and the change range of the response value. As shown in Fig. 5, the effect of temperature on the response value was the greatest. With the temperature increasing, the generated oil deoxygenation was the first to increase and then stabilize. At the same temperature, the deoxygenation increased with increasing pressure, but it decreased with increasing pressure at higher temperatures. The deoxygenation increased first and then tended to be constant with increasing reaction time, but it was found that the yield of produced oil decreased and coke increased with increasing reaction time during the experiment.

The data of 29 experiments were statistically analyzed by Design-Expert 8.0.6.1 software to obtain the optimum conditions for four factors. The optimum reaction conditions were a temperature of 369.6 ℃, pressure of 2 MPa, time of 6.9 h, and catalyst amount of 0.22 g. In these conditions, the deoxygenation percentage of Jatropha oil was 95.1%.

Due to experimental constraints, the optimum parameters were modified to a temperature of 370 ℃, pressure of 2 MPa, time of 7 h, and catalyst amount of 0.22 g. Three parallel experiments were conducted, and the deoxygenation percentages of Jatropha oil were 94.9%, 95.3%, and 95.0%, with an average value of 95.1 %. Because this result was similar to the predicted value, the model was reliable.

Generating Oil Composition Analysis

Jatropha oil contains 78.9% unsaturated acids (Sarin *et al.* 2007) with a high oxygen content, and the resulting oil obtained by catalytic deoxygenation has a significantly lower oxygen content. It consists mainly of C7-C20 hydrocarbons (>80%) and a small amount of oxygenated compounds (<16%).

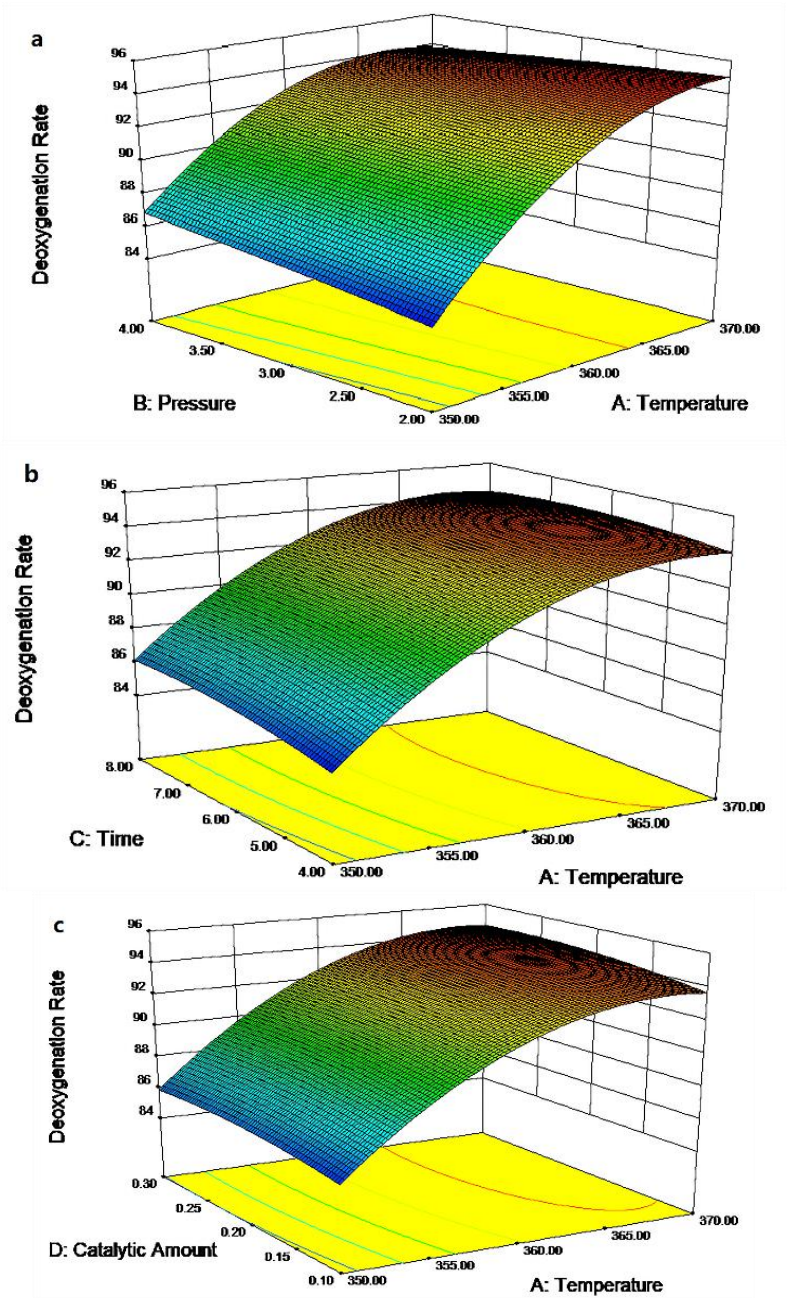

Fig. 5. Response surface curves for different variables

Figure 6 shows the content of oxygenated compounds decreased with increasing hydrogen pressure at the same temperature. As the content of isoparaffins increased, the content of straight chain alkanes increased, and the content of cycloalkanes and olefins decreased. The content of C8-C16 at different hydrogen pressures was above 60%. The generated oil contained a large amount of aviation kerosene components. The Py-IR analysis shows that WO_3-ZrO_2 was a solid acid catalyst containing Brönsted and Lewis acid sites. The interaction of the triglyceride molecule with the surface Lewis acid can largely promote the activation of the C-O bond and inhibit the cleavage of the C-C bond. The data in Fig. 7 show that no isoalkanes were produced at hydrogen pressure of 1 MPa, and the isoalkanes increased and then decreased with increasing hydrogen pressure. Pérez

et al. (2017) suggested that saturated isomeric alkanes may be formed by hydroisomerization of olefins, and the isomerization process depends on Lewis acid sites (Juan *et al.* 2018). Han *et al.* (2011) suggested that weak and medium acid sites are favorable for isomerization reactions, and the key step is the formation of branched alkylcarbonium ions. The increase of isomeric alkanes was beneficial to increase the fluidity of the generated oil at low temperature and to reduce the viscosity of the generated oil, which has an important role in improving the quality of aviation kerosene.

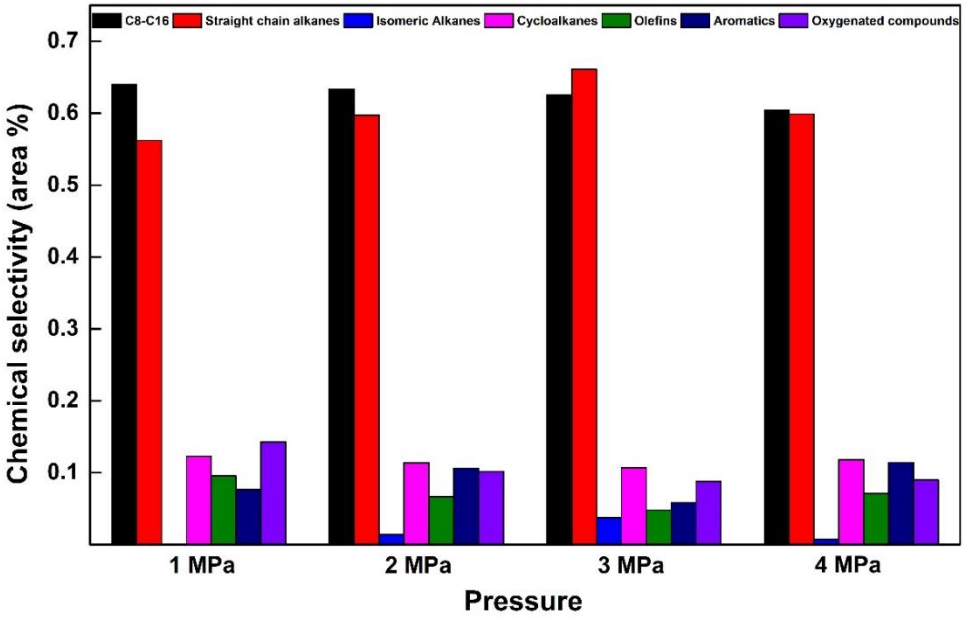

Fig. 6. Distribution of product components of oil generated at different pressures at 360 °C

As shown in Fig. 7, the deoxygenation percentage of jatropha oil increased with the increase of temperature, while the effect of pressure on the deoxygenation of jatropha oil was not obvious. With the increase of temperature, the content of oxygenated compounds decreased, and the content of straight-chain alkanes and cycloalkanes increased. C8-C16 was mainly obtained from C15-C18 by C-C bond cleavage during the reaction process. The increase of temperature was favorable to the C-C bond cleavage, and some long-chain alkanes were broken into short-chain alkanes, making the content of C8-C16 increase. The content of C7-C18 alkanes in the generated oil was 90.34%, 90.74%, and 90.30% with the increase of temperature, respectively. Among the alkanes, C7-C14/C15-C18 were 0.87, 0.95, and 1.45, respectively, and the ratio increased with the increase of temperature. This data suggests that there was a cleavage of long-chain alkanes into short-chain alkanes, which showed a positive correlation with the strong acid site of the catalyst, indicating that the strong acid site favors the cleavage reaction (Peng *et al.* 2012; Shim *et al.* 2015). The isoparaffin content increased significantly at increasing temperature, reaching 12.0% at 370 °C and 14.2% at cyclic alkanes, with better mobility of the resulting oil. A certain amount of naphthenic hydrocarbons is beneficial to lower the freezing point of the generated oil, so that the generated oil still has good fluidity at lower temperatures and improves the quality of aviation kerosene.

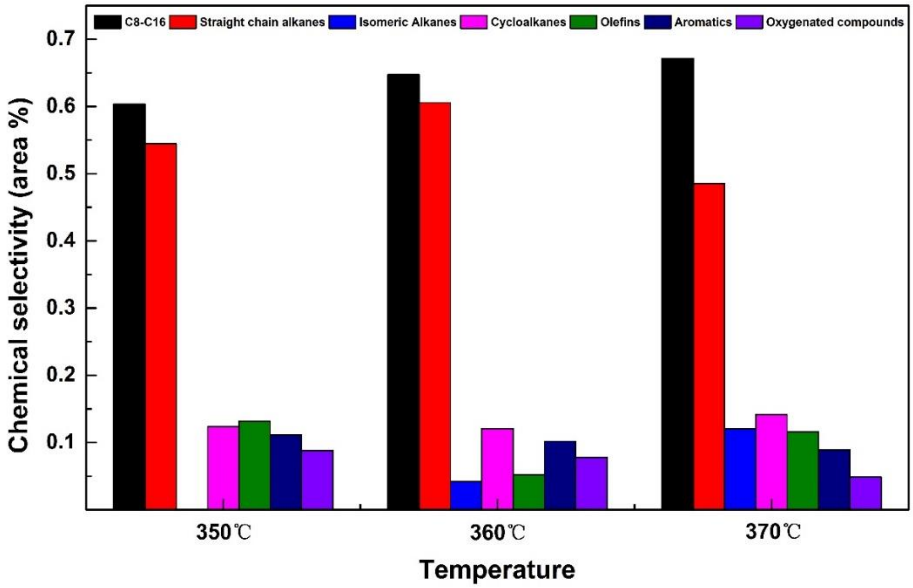

Fig. 7. Distribution of oil product fractions at different temperatures at 2 MPa

Table 7. Analysis of the Main Components of the Generated Oil

Grouping	Area (%)		
	350 °C	360 °C	370 °C
2,4-Dimethylheptane	-	-	6.49
Octane	4.01	4.04	-
Nonane	4.63	3.77	4.97
Decane	3.03	-	-
3,5-Dimethyloctane	-	3.42	4.51
Undecane	3.34	3.89	4.72
Dodecane	3.39	4.35	4.02
Tridecane	2.89	3.63	3.14
Tetradecane	2.72	3.74	2.94
Pentadecane	10.91	13.59	7.74
Heptadecane	3.01	4.11	2.73
Heptadecane	14.31	5.96	12.72
8-Heptadecene	3.48	0.54	1.31
n-Heptadecanol	-	0.29	1.36
Undecylcyclohexane	5.84	5.17	5.91
Octadecane	1.38	2.03	0.69
Dodecylbenzene	2.33	1.43	0.58
4-Dodecylphenol	4.57	1.94	1.08

As shown in Table 7, based on the product distribution obtained by GC-MS mass spectrometry, the main products obtained during the conversion of jatropha oil were straight chain alkanes from C8 to C17 (octane, nonane, undecane, dodecane, tridecane, tetradecane, pentadecane, hexadecane, heptadecane), 3,5-dimethyloctane, and

undecylcyclohexane. The predominantly saturated alkanes in the resulting oils indicate that the unsaturated C=C bonds in jatropha oils (*e.g.*, oleic and linoleic acids) were fully hydrogenated. The hydrocarbon content of the generated oil was mainly pentadecane and heptadecane, indicating a predominantly DCO/DCO_2 reaction (Mäki-Arvela *et al.* 2008; Hollak *et al.* 2012), with heptadecane as the major component, indicating a predominantly decarbonylated route of deoxygenation.

CONCLUSIONS

1. The prepared WO_3-ZrO_2 was characterized by X-ray diffraction (XRD), transmission electron microscopy (TEM), adsorption of cold nitrogen gas (BET), and pyridine adsorbed IR spectroscopy (Py-IR). The results showed that 15% WO_3-ZrO_2 solid acid catalyst was well prepared, and the introduction of WO_3 provided a Brönsted acid site for ZrO_2.
2. The order of the effect of WO_3-ZrO_2 on the deoxygenation of the generated oil was obtained by response surface methodology: reaction temperature > catalyst amount > reaction time > reaction pressure. The optimum reaction conditions were a temperature of 370 ℃, pressure of 2 MPa, time of 7 h, and catalyst amount of 0.22 g. Under the optimal conditions, the deoxygenation percentage of the generated oil was 95.1%, which was close to the theoretical value, showing that the model is reliable.
3. The catalytic deoxygenation effect of WO_3-ZrO_2 on Jatropha oil was mainly affected by temperature. The C8-C16 content of the resulting oil obtained by the GC-MS area normalization method under the optimal conditions was 68.1%, and the isoparaffin content was 12.0%. The naphthenic content was 14.2%, the aromatic compound is 8.91%, and it contained a large amount of aviation kerosene components.

ACKNOWLEDGMENTS

This work was supported by the Hainan Provincial Department of Science and Technology (ZDYF2018134) and the College of Chemical Engineering, Hainan University, Haikou, Hainan, China. The authors are grateful for the valuable comments from the reviewers and editors to improve the quality of this paper.

REFERENCES CITED

Abdulgader, M., Yu, J., Zinatizadeh, A.A., Williams, P., and Rahimi, Z. (2019). "Process analysis and optimization of single stage flexible fibre biofilm reactor treating milk processing industrial wastewater using response surface methodology (RSM)," *Chem. Eng. Research and Design* 149, 169-181. DOI: 10.1016/j.cherd.2019.07.011

Dedsuksophon, W., Faungnawakij, K., Champreda, V., and Laosiripojana, N. (2011). "Hydrolysis/dehydration/aldol-condensation/hydrogenation of lignocellulosic biomass and biomass-derived carbohydrates in the presence of Pd/WO_3–ZrO_2 in a single reactor," *Bioresource Technology* 102(2), 2040-2046. DOI: 10.1016/j.biortech.2010.09.073

Doliente, S. S., Narayan, A., Tapia, J. F. D., Samsatli, N. J., Zhao, Y., and Samsatli, S. (2020). "Bio-aviation fuel: A comprehensive review and analysis of the supply chain components," *Frontiers in Energy Research* 8, 110. DOI: 10.3389/fenrg.2020.00110

Gosselink, R. W., Hollak, S. A., Chang, S.W., van Haveren, J., de Jong, K. P., Bitter, J. H., and van Es, D. S. (2013). "Reaction pathways for the deoxygenation of vegetable oils and related model compounds," *ChemSusChem* 6(9), 1576-1594. DOI: 10.1002/cssc.201300370

Halim, S. F. A., Kamaruddin, A. H., and Fernando, W. (2009). "Continuous biosynthesis of biodiesel from waste cooking palm oil in a packed bed reactor: Optimization using response surface methodology (RSM) and mass transfer studies," *Bioresource Technology* 100(2), 710-716. DOI: 10.1016/j.biortech.2008.07.031

Han, J., Duan, J., Chen, P., Lou, H., Zheng, X., and Hong, H. (2011). "Nanostructured molybdenum carbides supported on carbon nanotubes as efficient catalysts for one-step hydrodeoxygenation and isomerization of vegetable oils," *Green Chemistry* 13(9), 2561-2568. DOI: 10.1039/c1gc15421d

Hollak, S.A., Bitter, J.H., van Haveren, J., de Jong, K.P., and van Es, D.S. (2012). "Selective deoxygenation of stearic acid via an anhydride pathway," *RSC Advances* 2(25), 9387-9391. DOI: 10.1039/c2ra21651e

Islam, A. K. M. A., Primandari, S. R. P., and Yaakob, Z. (2018). "Non-edible vegetable oils as renewable resources for biodiesel production: South-East Asia perspective," *Advances in Biofuels and Bioenergy*, Ch. 10, pp. 201-215. DOI: 10.5772/intechopen.73304

Jing, G., Li, J., Yang, D., and Hao, J. (2009). "Promotional mechanism of tungstation on selective catalytic reduction of NOx by methane over In/WO_3/ZrO_2," *Applied Catalysis B: Environmental* 91(1-2), 123-134. DOI: 10.1016/j.apcatb.2009.05.015

Juan, I., Cardeño, F., Pérez, W., Peña, J.D., and Rios, L.A. (2018). "Catalytic hydrotreating of jatropha oil into non-isomerized renewable diesel: Effect of catalyst type and process conditions," *Chem. Eng. J.* 352, 232-240. DOI: 10.1016/j.cej.2018.07.021

Kim, S., Lauterbach, J., and Sasmaz, E. (2021). "Yolk–shell Pt-NiCe@ SiO_2 single-atom-alloy catalysts for low-temperature dry reforming of methane," *ACS Catalysis* 11(13), 8247-8260. DOI: 10.1021/acscatal.1c01223

Kumar, R., Rana, B. S., Tiwari, R., Verma, D., Kumar, R., Joshi, R. K., Garg, M.O., and Sinha, A. K. (2010). "Hydroprocessing of jatropha oil and its mixtures with gas oil," *Green Chemistry* 12(12), 2232-2239. DOI: 10.1039/c0gc00204f

Lee, Y., Shafaghat, H., Kim, J.-k., Jeon, J.-K., Jung, S.-C., Lee, I.-G., and Park, Y.-K. (2017). "Upgrading of pyrolysis bio-oil using WO_3/ZrO_2 and Amberlyst catalysts: Evaluation of acid number and viscosity," *Korean Journal of Chemical Engineering* 34(8), 2180-2187. DOI: 10.1007/s11814-017-0126-x

Lercher, J.A., Gründling, C., and Eder-Mirth, G. (1996). "Infrared studies of the surface acidity of oxides and zeolites using adsorbed probe molecules," *Catalysis Today* 27(3-4), 353-376. DOI: 10.1016/0920-5861(95)00248-0

Li, W., Wang, H., Wu, X., Betancourt, L.E., Tu, C., Liao, M., Cui, X., Li, F., Zheng, J., and Li, R. (2020). "Ni/hierarchical ZSM-5 zeolites as promising systems for phenolic bio-oil upgrading: Guaiacol hydrodeoxygenation," *Fuel* 274. DOI: 10.1016/j.fuel.2020.117859

Mäki-Arvela, P., Snåre, M., Eränen, K., Myllyoja, J., and Murzin, D. Y. (2008). "Continuous decarboxylation of lauric acid over Pd/C catalyst," *Fuel* 87(17-18), 3543-3549. DOI: 10.1016/j.fuel.2008.07.004

Mortensen, P. M., Grunwaldt, J.-D., Jensen, P.A., Knudsen, K., and Jensen, A.D. (2011). "A review of catalytic upgrading of bio-oil to engine fuels," *Applied Catalysis A: General* 407(1-2), 1-19. DOI: 10.1016/j.apcata.2011.08.046

Nygren, E., Aleklett, K., and Höök, M. (2009). "Aviation fuel and future oil production scenarios," *Energy Policy* 37(10), 4003-4010. DOI: 10.1016/j.enpol.2009.04.048

Patel, M., and Kumar, A. (2016). "Production of renewable diesel through the hydroprocessing of lignocellulosic biomass-derived bio-oil: A review," *Renewable and Sustainable Energy Reviews* 58, 1293-1307. DOI: 10.1016/j.rser.2015.12.146

Pattnaik, F., Nanda, S., Kumar, V., Naik, S., and Dalai, A.K. (2021). "Subcritical water hydrolysis of Phragmites for sugar extraction and catalytic conversion to platform chemicals," *Biomass and Bioenergy* 145, article no. 105965. DOI: 10.1016/j.biombioe.2021.105965

Peng, B., Yao, Y., Zhao, C., and Lercher, J. A. J. A. C. I. E. (2012). "Towards quantitative conversion of microalgae oil to diesel-range alkanes with bifunctional catalysts," *Angewandte Chemie Int. Ed.* 51(9), 2072-2075. DOI: 10.1002/anie.201106243

Pérez, W., Marín, J., del Río, J., Peña, J., and Rios, L. (2017). "Upgrading of palm oil renewable diesel through hydroisomerization and formulation of an optimal blend," *Fuel* 209, 442-448. DOI: 10.1016/j.fuel.2017.08.013

Piva, D., Piva, R., Pereira, C., Silva, D., Montedo, O., Morelli, M., and Urquieta-González, E. (2020). "Facile synthesis of WOx/ZrO_2 catalysts using $WO_3 \cdot H_2O$ precipitate as synthetic precursor of active tungsten species," *Materials Today Chemistry* 18, article no. 100367. DOI: 10.1016/j.mtchem.2020.100367

Qian, E.W., Chen, N., and Gong, S. (2014). "Role of support in deoxygenation and isomerization of methyl stearate over nickel–molybdenum catalysts," *Journal of Molecular Catalysis A: Chemical* 387, 76-85. DOI: 10.1016/j.molcata.2014.02.031

Salgado, A. L. P., Araújo, F. C., Soares, A. V., Xing, Y., and Passos, F. B. J. A. C. A. G. (2021). "Glycerol hydrogenolysis over Ru-Cu bimetallic catalysts supported on modified zirconias," *Applied Catalysis A: General* 626, article no. 118359. DOI: 10.1016/j.apcata.2021.118359

Samy, M., Ibrahim, M. G., Alalm, M. G., Fujii, M., Ookawara, S., and Ohno, T. (2020). "Photocatalytic degradation of trimethoprim using S-TiO_2 and Ru/WO_3/ZrO_2 immobilized on reusable fixed plates," *Journal of Water Process Engineering* 33, article no. 101023. DOI: 10.1016/j.jwpe.2019.101023

Sarin, R., Sharma, M., Sinharay, S., and Malhotra, R. K. (2007). "Jatropha–palm biodiesel blends: An optimum mix for Asia," *Fuel* 86(10-11), 1365-1371. DOI: 10.1016/j.fuel.2006.11.040

Shim, J.-O., Jeong, D.-W., Jang, W.-J., Jeon, K.-W., Kim, S.-H., Jeon, B.-H., Roh, H.-S., Na, J.-G., Oh, Y.-K., and Han, S.S. (2015). "Optimization of unsupported CoMo catalysts for decarboxylation of oleic acid," *Catalysis Communications* 67, 16-20. DOI: 10.1016/j.catcom.2015.03.034

Shkurenok, V., Smolikov, M., Kir'yanov, D., and Belyi, A. (2021). "Isomerization of alkanes over bifunctional Pt (Pd)/WO_3-ZrO_2 catalysts," *AIP Conference Proceedings* Vol. 2412, No. 1, p., 020011. DOI: 10.1063/5.0075226

Stepacheva, A. A., Markova, M. E., Schipanskaya, E. O., Matveeva, V. G., and Sulman, M. G. (2021). "Highly effective schungite-based catalyst for deoxygenation of biomass components," *Chem. Eng. Trans.* 88, 283-288. DOI: 10.3303/CET2188047

Tang, H., Lin, J., Cao, Y., Jibran, K., and Li, J. (2022). "Influence of NiMoP phase on hydrodeoxygenation pathways of jatropha oil," *Energy* 243, article no. 123048. DOI:

10.1016/j.energy.2021.123048
Tong, Q., Zong, A., Gong, W., Yu, L., and Fan, Y. (2016). "Rhenium-promoted Pt/WO_3/ZrO_2: An efficient catalyst for aqueous glycerol hydrogenolysis under reduced H_2 pressure," *RSC Advances* 6(89), 86663-86672. DOI: 10.1039/c6ra21198d
Verma, D., Rana, B.S., Kumar, R., Sibi, M., and Sinha, A.K. (2015). "Diesel and aviation kerosene with desired aromatics from hydroprocessing of jatropha oil over hydrogenation catalysts supported on hierarchical mesoporous SAPO-11," *Applied Catalysis A: General* 490, 108-116. DOI: 10.1016/j.apcata.2014.11.007
Wang, H., Male, J., and Wang, Y. (2013). "Recent advances in hydrotreating of pyrolysis bio-oil and its oxygen-containing model compounds," *ACS Catalysis* 3(5), 1047-1070. DOI: 10.1021/cs400069z
Wang, Z. (2019). "Does biomass energy consumption help to control environmental pollution? Evidence from BRICS countries," *Science of the Total Environment* 670, 1075-1083. DOI: 10.1016/j.scitotenv.2019.03.268
Wang, S., Cao, M., Sun, S., Jiang, H., Duan, Y., Kong, X., and Wang, H. (2020a). "Selective hydroisomerization of isobutane to n-butane over WO_3-ZrO_2 supported Ni-Cu alloy," *Fuel* 280, article no. 118274. DOI: 10.1016/j.fuel.2020.118274
Wang, S., Cao, M., Sun, S., Jiang, H., Duan, Y., Kong, X., and Wang, H. (2020b). "Selective hydroisomerization of isobutane to n-butane over WO_3-ZrO_2 supported Ni-Cu alloy," *Fuel* 280, article no. 118274. DOI: 10.1016/j.fuel.2020.118274
Xiao, Y., Yi, X., Peng, W., Chen, W., Liu, Z., and Zheng, A. (2021). "Precisely regulating the Brønsted acidity and catalytic reactivity of novel allylic C–H acidic catalysts," *Fuel* 289, article no. 119845. DOI: 10.1016/j.fuel.2020.119845
Xu, Y., Ramanathan, V., and Victor, D. G. (2018). "Global warming will happen faster than we think," *Nature* 564, 30-32.
Yang, F., and Dian, J. (2022). "Macro-economic impact of policies for controlling fossil energy consumption in China," *Energies* 15(3), article no. 1051. DOI: 10.3390/en15031051
Yang, H., Du, X., Lei, X., Zhou, K., Tian, Y., Li, D., and Hu, C. (2021). "Unraveling enhanced activity and coke resistance of Pt-based catalyst in bio-aviation fuel refining," *Applied Energy* 301, article no. 117469. DOI: 10.1016/j.apenergy.2021.117469
Zacher, A. H., Olarte, M. V., Santosa, D. M., Elliott, D. C., and Jones, S. B. (2014). "A review and perspective of recent bio-oil hydrotreating research," *Green Chemistry* 16(2), 491-515. DOI: 10.1039/c3gc41382a
Zerva, C., Karakoulia, S. A., Kalogiannis, K. G., Margellou, A., Iliopoulou, E. F., Lappas, A. A., Papayannakos, N., and Triantafyllidis, K. S. (2021). "Hydrodeoxygenation of phenol and biomass fast pyrolysis oil (bio-oil) over Ni/WO_3-ZrO_2 catalyst," *Catalysis Today* 366, 57-67. DOI: 10.1016/j.cattod.2020.08.029
Zhu, T., Zhang, L., Li, Z., Wei, G., Xin, Z., Xiong, D., and Ou, Z. (2021). "Partial hydrogenation of Jatropha oil biodiesel catalyzed by nickel/Bentonite catalyst," *Waste and Biomass Valorization* 12(1), 465-474. DOI: 10.1007/s12649-020-00977-8

Article submitted: June 7, 2022; Peer review completed: June 25, 2022; Revised version received and accepted: August 3, 2022; Published: August 12, 2022.
DOI: 10.15376/biores.17.4.5679-5694